Available online at www.sciencedirect.com
SCIENCE DIRECT®
International Journal of Pharmaceutics 298 (2005) 293–304
international journal of pharmaceutics
www.elsevier.com/locate/ijpharm

Role of gut macrophages in mice orally contaminated with scrapie or BSE

Thomas Maignien [a,1], Monjed Shakweh [b,1], Pilar Calvo [b], Dominique Marcé [a], Nicole Salès [a,c], Elias Fattal [b], Jean-Philippe Deslys [a], Patrick Couvreur [b,*], Corinne Ida Lasmezas [a]

[a] *CEA, Service de Neurovirologie, CRSSA, B.P.6, Fontenay-aux-Roses Cedex, France*
[b] *Université Paris-Sud, Centre d'Etudes Pharmaceutiques, UMR CNRS 8612, 5 rue Jean-Baptiste Clément, 92296 Chatenay-Malabry Cedex, France*
[c] *Université de Caen, UFR des Sciences Pharmaceutiques, Bd Bécquerel, 14032 Caen Cedex, France*

Received 3 January 2005; received in revised form 10 February 2005; accepted 20 February 2005

Abstract

While there is a growing consensus on the understanding of the propagation pathways after oral infection of transmissible spongiform encephalopathy (TSE) agents and even if the central role of follicular dendritic cells is identified, little is known about the key players in the first steps of the infection and about the site of the disease development. We investigated the role of gut macrophages, which are capable of capturing aggregates of the prion protein. PLGA particles containing clodronate were designed in order to be orally administered and to target Peyer's patches for inducing gut-associated macrophages suicide in mice. Mice were subsequently infected with scrapie or BSE by the oral route. It was found that the efficacy of macrophage suppression in the Peyer's patches correlated well with an earlier appearance of PrPres in these formations and with a higher amount of PrPres at a later stage of the infection. Thus, the capture of infectious particles that have crossed the epithelial gut barrier and their elimination by macrophages seems to be a key event to restrict the amount of agent initiating the infection.

Keywords: Transmissible spongiform encephalopaties; Macrophage-suicide technique; Clodronate; Peyer's patches; Intestinal uptake; Nano- and microparticles

1. Introduction

Transmissible spongiform encephalopathies (TSE), also called prion diseases, are fatal neurodegenerative diseases, a number of which are due to oral contamination with the infectious agent. Bovine spongiform

* Corresponding author. Fax: +33 1 46 61 93 34.
E-mail address: patrick.couvreur@cep.u-psud.fr (P. Couvreur).
[1] Equal contribution.

0378-5173/$ – see front matter © 2005 Elsevier B.V. All rights reserved.
doi:10.1016/j.ijpharm.2005.02.042

encephalopathy (BSE) affects cattle which have been fed with infected meat and bone meal. More recently, the BSE agent has been passed to humans through the alimentary chain causing variant Creutzfeldt–Jakob Disease (Bruce et al., 1997, Hill et al., 1997, Lasmezas et al., 2001; Will et al., 1996).

The involvement of the lymphoreticular system (LRS) in the pathogenesis of oral infection has been demonstrated in different experimental models either by searching directly for infectivity by bioassay, or by using PrPres as the biochemical marker for the agent replication (Beekes and McBride, 2000; Kimberlin and Walker, 1989; Sigurdson et al., 1999). Following infection of mice with BSE or scrapie, the kinetics and paths of agent propagation have been determined (Maignien et al., 1999): after a primary replication phase in the gut-related lymphoid tissue Peyer's patches and mesenteric lymph nodes, the agent recirculates through the lymph and blood and reaches more distal LRS organs, such as the spleen and the axillary lymph nodes, before the CNS is finally invaded. An alternative, more direct neuroinvasion route from the enteric nervous system exists too (Beekes and McBride, 2000; McBride and Beekes, 1999; van Keulen et al., 1999).

There are still some uncertainties concerning the cells involved in the first steps of the infection after oral contamination. Follicular dendritic cells (FDCs) of the Peyer's patches certainly support the agent replication as they do after intraperitoneal infection (Brown et al., 1999; Kitamoto et al., 1991; Mabbott et al., 2000; McBride et al., 1992; Montrasio et al., 2000) but they do not migrate and cannot account for the transport of infectivity from the intestinal lumen to the Peyer's patches nor to more distal LRS tissues. The involvement of the B lymphocyte, in particular as an actor in FDC maturation, has been shown in detail (Brown et al., 1999; Klein et al., 1997; Montrasio et al., 2001). Attention has been focused on macrophages too, as they express PrPc at the plasmic membrane and can be long-lived and radioresistant, features of cells able to support TSE agents replication (Fraser et al., 1989). They can capture some infectivity in vitro, and sequester appreciable levels of infectivity and PrPres in vivo (Jeffrey et al., 2000; Manuelidis et al., 2000). These observations support a role of macrophages in the pathogenesis of TSEs. One of our studies pointed towards the involvement of macrophages as scavengers after intraperitoneal infection (Beringue et al., 2000).

In this study, we took advantage of our knowledge on the pathogenesis of the oral infection of the C57BL/6 mouse with scrapie or BSE (Maignien et al., 1999) and used the "macrophage-suicide technique" (Van Rooijen, 1989) to study if a targeted destruction of the gut macrophage population would alter the replication of the agent in its first ecological niches of the digestive tract, i.e. the Peyer's patches (PPs). As the PPs were, indeed, described as the primary site of particles uptake after oral administration (Eldridge et al., 1990, Jani et al., 1989; McClean et al., 1998), we used this approach for selective macrophages killing. However, despite the large amount of literature concerning particle uptake by PPs, optimal physicochemical characteristics for efficient PPs uptake, are not yet clearly defined (Shakweh et al., 2004). This is the reason why the optimal size of the particle taken up by PPs were also tested in this paper, using fluorescent nano- and microspheres made of poly(lactide-co-glycolide) acid (PLGA).

2. Materials and methods

2.1. Materials

2.1.1. Chemical products

Poly(DL-lactide-co-glycolide) (PLGA, Resomer® RG 756, MW 98,000 Da, copolymer ratio 75:25) was purchased from Boehringer Ingelheim (Germany). Poly(vinyl alcohol) (PVA, average MW 30,000–70,000), rhodamine-6G were all obtained form Sigma Chemical (France). Clodronate (or Dichloro methylen biphosphonate, Cl_2MBP) was generously supplied by Roche Diagnostic (Germany).

2.1.2. Antibodies

Primary antibodies used for immunohistchemistry included rat anti-mouse monoclonal antibodies: anti-CD45R/B220 (clone RA3-6B2, Pharmingen), anti-FDC (clone FDC-M1, provided by Marie Kosco-Vilbois, Geneva Biomedical Research Institute), Anti-F4/80 (Serotec) and Hamster Anti-Mouse CD3e (Pharmingen). Secondary antibodies used were biotinylated polyclonal goat anti-rat IgG (Pharmingen), biotinylated mouse anti-hamster cocktail (Pharmingen) and peroxidase-conjugated goat anti-rat IgG (serotec).

2.1.3. Animals and TSE agent strains

The experiments of nano- and microspheres uptake by PPs were performed in C57BL/6 mice acquired from R. Janvier (Le Genest-Saint-Isle, France). The murine C506M3 strain is derived from a natural case of sheep scrapie (a kind gift from P. Brown, NIH, Bethesda, USA). It was passaged tenfold in C57BL/6 mice and has an LD50 titre of $10^{8.9}$/g of brain. The murine 6PB1 clonal strain is derived from the 4PB1 BSE strain isolated in C57BL/6 mice, which has an LD50 titre of $10^{9.3}$/g of brain (Lasmezas et al., 1996). Both strains have been characterized as intracerebral and i.p. infection models (Lasmezas et al., 1996).

2.2. Methods

2.2.1. Preparation of nano- and microparticles containing rhodamine or clodronate

Microparticles of various sizes were prepared by the water-in-oil-in-water (W1/O/W2) emulsion solvent evaporation technique. In all preparations, 0.1 ml of a water solution containing rhodamine 6G (25 μg rhodamine/mg polymer) or clodronate (100 μg clodronate/mg polymer) was added to a methylene chloride solution of PLGA at 25 and 100 mg/ml and submitted to vortex for 30 s. This primary emulsion was then placed in an ice bath and emulsified using a 10 mm probe sonication set at 40 W of energy output (CV154, Sonics & Materials, USA) for 60 s. Then, the emulsion was added to an aqueous solution (10 or 50 ml) containing PVA (2%) and NaCl (5%) with intermittent vortexing for 30 s to obtain the final multiple emulsion. This emulsion was then placed in an ice bath and sonicated for an average particle size of 0.3 or 1 μm or homogenized with the aid of an Ultraturrax (8000 rpm; 1 min) (Janke & Kunnkel, T25, Germany) when the desired mean diameter was 3 μm (Table 1). The emulsion was finally stirred overnight using a mechanical stirring plate to allow solvent evaporation. Particle suspension was centrifuged at 5333 × *g* (centrifuge Jouan Model CR412) for 2 h for particles of expected mean diameter of 0.3 μm and 30 min or 15 min for particles of expected mean size of 1 and 3 μm, respectively. The pellet was then suspended in distilled water and centrifuged. This washing step (repeated three times) was carried out to remove the excess of PVA and the non encapsulated rhodamine-6G or clodronate. At least, 12.5 mg and/or 50 mg D-glucose used as cryoprotector

Table 1
Physicochemical properties of nano- and microparticles of PLGA

Desired diameter (μm)	PLGA (%)		O:W2	Emulsion (W1/O/W2)	Time (min)	Actual diameter (μm)			Preparation yield (%)	Zeta potential (mV)	Encapsulation efficiency (μg clodronate/mg of particle
						D_{10}	D_{50}	$^2D_{90}$			
3	10	PLGA-rhodamine 6G	1:10	Homogeniser	2	2.4	3.3	4.4	77.8 ± 6.5	−33.7 ± 4.9	
		PLGA-clodronate	1:10			2.7	3.6	4.6	82.6 ± 5.1	−29.8 ± 1.1	27.2 ± 4.3
1	10	PLGA-rhodamine 6G	1:2	Probe sonication	1	0.7	1.0	1.3	61.7 ± 2.4	−31.9 ± 3.8	
		PLGA-clodronate	1:2			0.8	1.1	1.4	63.8 ± 1.4	−28.4 ± 2.7	18.9 ± 2.1
						Mean size	^{3}PI				
0.3	2.5	PLGA-rhodamine 6G	1:2	Probe sonication	2	0.28	0.08		49.5 ± 3.2	−30.1 ± 2.2	
		PLGA-clodronate	1:2		2	0.31	0.11		52.7 ± 3.8	−27.3 ± 3.3	5.1 ± 1.2

$^2D_{90}$: refers that 90% of microparticles have a size less than indicated values, ^{3}PI: polydispersity index.

were added to nano- and microparticles, respectively suspended in 5 ml of distilled water before particles were submitted to freeze-drying for 48 h (freeze-drier Modele CHRIST Alpha 1–4, BIOBLOCK SCIENTIFIC).

2.2.2. Particle size and zeta potential analysis

Nanoparticle mean size and size distribution were analyzed by photon correlation spectroscopy using the quasi-elastic light scattering method (Coulter Nanosizer N4 plus, USA). Particles with a mean diameter $\geq 1\,\mu m$ were sized by laser diffractometry (Beckman Coulter LS 100Q, USA). Microparticle size was expressed as a volume diameter. Measurements of PLGA particle zeta potential, suspended in a 1 mM KCl solution, were carried out at 25 °C using a Zetasizer-4 (Malvern Instruments, UK).

2.2.3. Scanning electron microscopy (SEM)

Samples were prepared from dilutions in distilled water of particle suspensions and dropped onto stubs. After air-drying, particles were coated with a thin layer of chrome and then examined by scanning electron microscopy (LEO 1530, France).

2.2.4. Clodronate encapsulation

Clodronate associated with PLGA nano- and microparticles was quantified by the method of complexation with cupper(II) sulphate. Practically, 5 mg of particles were at first degraded in 1 ml of NaOH 0.5 M. The resulting solution was then neutralized with 1 ml of 1 M acetic acid. The resulting solution (pH 5.0 ± 0.2) was diluted in acetate buffer (1:1) and then complexed with copper(II) in 0.1 M acetate buffer at pH 5.2. The absorbance value was measured by spectrophotometer at 235 nm (Perkin-Elmer UV–vis spectrophotometer, Lambda 11, USA). The amount of clodronate was then determined using a calibration curve performed in the same conditions.

2.2.5. Clodronate release from particles in artificial gastric and intestinal media (USP XXII)

The release of clodronate from nano- and microparticles was determined 1 h after incubation of the particles in a gastric medium (pH 1.2; 37 °C) followed up by a 48 h incubation in an intestinal medium (pH 7.5; 37 °C). These media were prepared as described in USP XXII. Simulated gastric fluid was prepared as follow: 2.0 g of sodium chloride and 3.2 g of pepsin were dissolved in 7.0 ml of hydrochloric acid and water was then added to reach a volume of 1000 ml. This test solution displayed a pH of about 1.2. To obtain the reconstituted intestinal fluid, 6.8 g of monobasic potassium phosphate were dissolved in 250 ml of distilled water. 190 ml of 0.2 N sodium hydroxide and 400 ml of water were then added. Finally, 10.0 g of pancreatin were added to the mixture. The pH of the resulting solution was adjusted to 7.5 ± 0.1 with 0.2 N sodium hydroxide. The final solution was diluted with water to 1000 ml.

To determine the kinetic profiles of clodronate release from PLGA particles, samples of each particle size (20 mg) were incubated in aliquots of 1 ml of the gastric media for at least 1 h at 37 °C. At each time point, the suspension was centrifuged at $5333 \times g$ (2 h). 0.5 ml of each supernatant sample was then added to 0.5 ml of 0.1 M acetate buffer containing 0.2 mg/ml of cupper(II) sulfate for spectrophotometric analysis (235 nm). One hour after incubation in gastric media, particle samples were then centrifuged at $5333 \times g$ (2 h), the supernatants were removed and the sediments were directly transferred to intestinal media and incubated for 48 h. At each time interval, the released clodronate from particles was quantified as follow: 0.5 ml of the supernatant was at first acidified with 0.5 ml of 1 M acetic acid. The final solution was diluted to an equal volume of an acetate buffer (0.1 M; pH 5.2) containing 0.2 mg/ml of copper(II) sulfate. The absorbance value of each solution was measured as described above. The amount of clodronate was then determined using a calibration curve realized in the same experimental conditions. The released clodronate was calculated and expressed as follows:

$$\text{Released clodronate (\%)} = \frac{\text{clodronate in supernatant (}\mu\text{g)}}{\text{total encapsulated clodronate (}\mu\text{g)}} \times 100$$

2.2.6. Animals, histological procedure and morphological analysis

Male mice, 5–7 weeks of age (average weight, 30 g) were fasted overnight before particle administration. 0.20 ml of a suspension of rhodamine containing particles (100 mg/ml) was administered to mice by direct gavage. Mice were then sacrified at time intervals (1, 4, 24 and 48 h). For morphological analysis, the

small intestine was divided into three equal segments. From the first segment one PP was sampled. Two PPs were sampled from the second and the third segments. Samples were then embedded in Cryomatrix® resin, frozen in liquid nitrogen. Finally, frozen samples were sectioned at a thickness of 10 μm for further observation by fluorescence microscopy. The semi-quantitative distribution of the number of fluorescent particles within the PPs cryosections was determined by epifluorescence using a Leitz microscope equipped with a filter for selective rhodamine excitation and connected to a Kappa CF 15/4 MCC camera video (Leica, Rueil Malmaison, France) sensitive to dim-light exposure. Images acquisition was achieved using the Photomat software (Microvision Instruments). Forty-five cryosections (from $n = 3$ animals) were examined per time point. The total observed area was 135,000 μm^2/animal. The number of fluorescent particles taken up by PPs was counted using Scion Image analysis software. Observations were carried out with a ×40 magnification for microparticles and with a ×100 magnification for nanoparticles.

As controls, non-treated animals with rhodamine-loaded particles or animals treated with rhodamine alone were sacrificed 1 and 24 h after treatment. These experiments allowed verification that the detected fluorescence in tissue was due to the presence of the fluorescent particles only. PBS administration allowed to distinguish between epithelium auto-fluorescence and the fluorescent resulting from the treatment.

2.2.7. Gut-associated macrophages depletion and oral contamination with TSE agents

Mice were treated twice with microspheres loaded with clodronate (of the same sizes as those tested for their uptake by PPs), 3 and 2 days before the oral contamination with the mouse-adapted scrapie (C506M3) strain. The total amount of clodronate administered per mouse was 2 mg. Animals were then orally contaminated with TSE agents as described by Maignien et al. (1999). For this purpose, the animals were placed in individual cages equipped with a liquid delivery system consisting of an Eppendorf tube pierced with a 3 mm hole. The tubes were filled with endolipid, a lipidic injectable emulsion for parenteral nutrition (composition: 20% soya oil, 1.2% egg lecithin, 2.5% glycerol in water) amenable to the preparation of an emulsion with brain homogenate that remains stable during the time of experimentation. Moreover, its appetizing properties encouraged rapid consumption by the animals. The next day, the tubes were filled with the infectious endolipid + brain preparation. Practically, 100 μl of 20% (w/v) scrapie or BSE brain homogenate were mixed with 100 μl endolipid. Consumption of the infectious preparations was carefully monitored; in all experiments described here, the mice drank the whole inoculum within 15 min. Fifty-six mice took the inoculum containing either of the two agent strains under monitoring.

Mice were then sacrificed by cervical dislocation at 60 and 130 days post-inoculation (p.i.), and PPs were harvested and kept at −80 °C until molecular analysis.

2.2.8. PrPres purification and detection

The tissues were homogenized at 20% (w/v) in a 5% sterile glucose solution. PrPres was then purified by centrifugation in the presence of detergents, after adapted proteinase K digestion according to a previously reported scrapie-associated fibril (SAF) protocol (Lasmezas et al., 1997). Samples were loaded on a 12% SDS polyacrylamide gel and then transferred onto a nitrocellulose membrane (Schleicher & Schuell). Immunoblotting was performed with a rabbit polyclonal anti-mouse PrP antibody (JB007, produced in the laboratory) at a 1/5000 dilution (Demaimay et al., 1997). Immunoreactivity was detected with an enhanced chemiluminescence kit (ECL, Amersham) and visualized on autoradiographic films. For each experiment, a dilution scale of the positive control, the brain of a C57BL/6 mouse at the terminal stage of the disease (C506M3 scrapie strain), was submitted to the same protocol for PrPres detection.

2.2.9. Immunohistochemistry

Freshly dissected tissue samples were embedded in Cryomatrix® compound and were frozen in liquid nitrogen. Cryostat sections were cut at 6 μm, thaw-mounted on Superfrost Plus® slides, air dried, and stored desiccated at −20 °C. Immediately before use, sections were fixed for 10 min in cold acetone containing 0.03% H_2O_2 to block endogenous peroxidase activity. Sections were rehydrated in PBS, blocked with 3% goat serum and 2% mouse serum in PBS containing 0.1% BSA for 30 min, and incubated with the primary antibodies diluted in PBS/0.1% BSA for 1 h at room temperature. Subsequently, sections were washed in

PBS and incubated with either peroxidase-conjugated goat anti-rat IgG or with biotinylated goat anti-hamster IgG followed by streptavidin-peroxidase. Bound peroxidase activity was visualized by incubating sections for 10 min in 3,3′-diaminobenzidine solution prepared upon supplier's specifications (Pharmingen, France). Sections were then counterstained with hematoxylin and dehydrated through four changes of increasing grades of alcohol to 100%, cleared in four changes of xylene and coversliped. Photographs were taken using a Leitz microscope connected to Kappa CF 15/4 MCC camera video (Leica, Rueil Malmaison, France). Images acquisition was achieved using the Photomat software (Microvision Instruments).

3. Results and discussion

3.1. Characterization of PLGA particles containing rhodamine and/or clodronate

Nano- and microparticles in the size range of 0.3, 1 and 3–5 μm were produced under optimised formulation conditions (Table 1). The following preparation conditions were varied (i) the co-polymer concentration in the organic phase; (ii) the ratio of the volume of the organic phase to the volume of the aqueous external phase (O/W2); and (iii) the emulsification technique to obtain the double emulsion (probe sonication or Ultraturrax). When the amount of emulsifier (PVA) was fixed, it was possible to obtain nanoparticles of a diameter of 0.3 μm using a PLGA concentration of 2.5%, a (O:W2) ratio of 1:2 and a sonication time of 1 min. Increasing the PLGA concentration to 10% allowed particles of larger size, around 1 μm to be produced. Finally, when the Ultraturrax was used to obtain the double emulsion, all particles displayed a diameter of 3–5 μm.

The preparation yield was in the same range for the three different types of particles, starting from 50% and raising to 80% as the size increased. It was observed that the introduction of clodronate did not influence particle size.

As shown in Table 1, the zeta potential of these particles was negative and the quantity of the encapsulated clodronate was found to be strongly size-dependant, since the larger the size the more efficient the encapsulation.

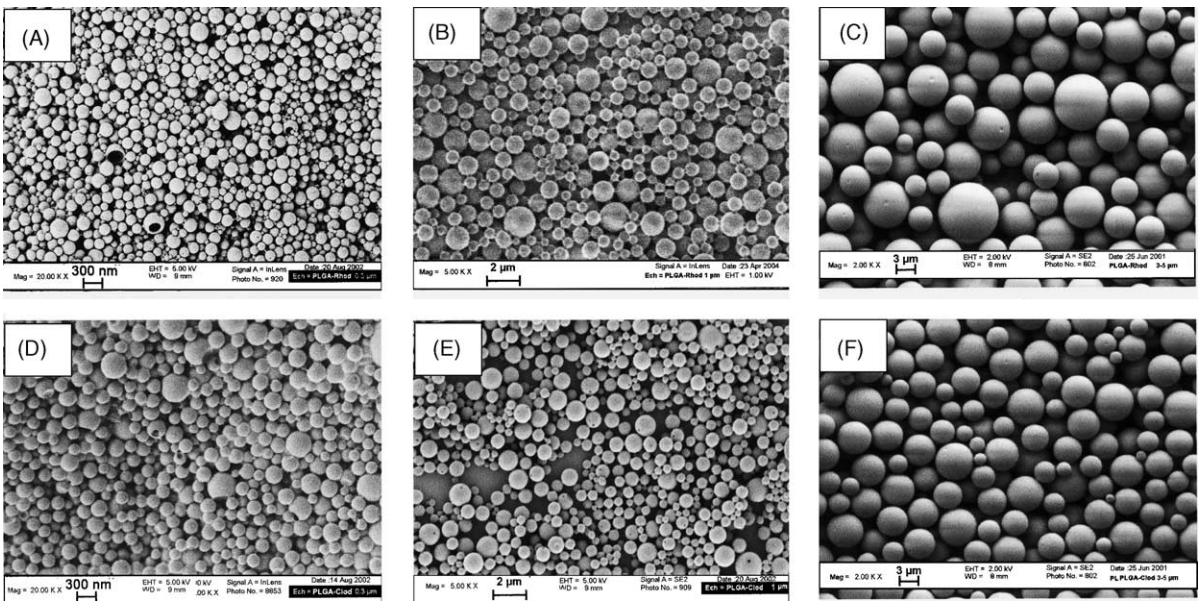

Fig. 1. Nano- and microspheres of PLGA analysed by scanning electron microscopy. (A)–(C) Rhodamine-loaded nano- and microspheres with a mean diameter of 0.3, 1 and 3–5 μm, respectively. (D)–(F) Clodronate-loaded nano- and microspheres with a mean diameter of 0.3, 1 and 3–5 μm, respectively.

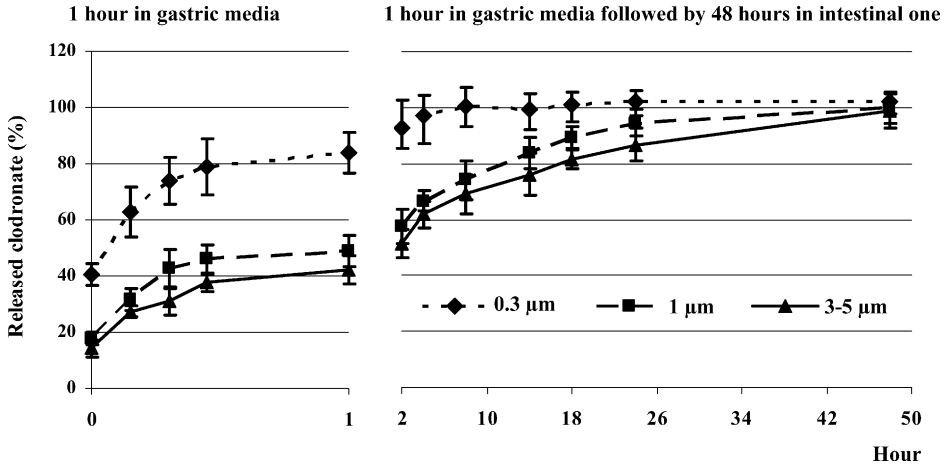

Fig. 2. Kinetic of clodronate release from nano- and microspheres of PLGA after incubation in gastric medium (1 h) followed by incubation in intestinal medium (48 h).

Scanning electron microscopy observation of nano- and microparticles revealed spherical structures with smooth surfaces. The morphological appearance of rhodamine- and/or clodronate-loaded nano- and microparticles was the same (Fig. 1).

The rate of clodronate release from nano- and microparticles with different sizes is shown in Fig. 2. Clodronate was completely released from the nanoparticles (0.3 μm) after 1 h of incubation in gastric fluid followed by 1 h in intestinal media at 37 °C. It is likely that the larger particles protect encapsulated clodronate more effectively since only 40–60% of the encapsulated clodronate were released from particles of 1 and 3–5 μm for the same periods, respectively. This may be explained by the fact that the smaller the particles are the larger is their specific surface area. Moreover, 14 h after incubation, 10–20% of clodronate still remained associated with the particles of 1 and 3–5 μm, respectively. However, 100% of encapsulated clodronate were released from particles whatever their diameter 1 h after incubation in gastric fluid followed by 48 h in intestinal media (Fig. 2).

3.2. Uptake of particles by Peyer's patches

Fig. 3A and B show cryo-sections of Peyer's patches, sampled from non-treated animals and from those fed with rhodamine free solution. While control mucosa from unfed animals did not show any significant autofluorescence (Fig. 4A), the treated mucosa with a rhodamine solution displayed a fluorescence which was diffuse and not in a punctuate form (Fig. 4B). This fluorescence decreased significantly 24 h after oral administration, but remained diffuse (Fig. 4C). On the contrary, Fig. 4D–G show that the microspheres of 0.3 and 1 μm concentrated in the dome of the Peyer's patches. They were found in this tissue as soon as 1 h after ingestion and were still detectable after 48 h (Fig. 3). The uptake was size-dependent since the 3–5 μm diameter particles were significantly less concentrated in Peyer's patches (Fig. 4H and I) than

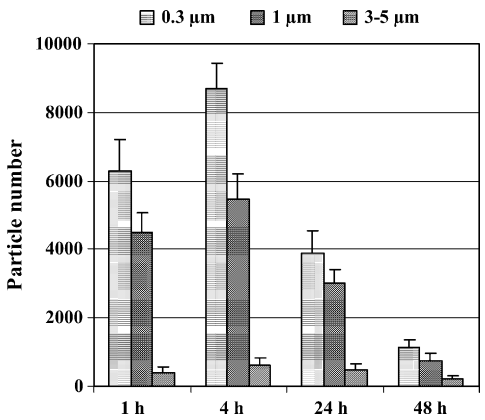

Fig. 3. Qualitative evaluation of the uptake, by Peyer's patches, of rhodamine-loaded nano- and microspheres after oral administration.

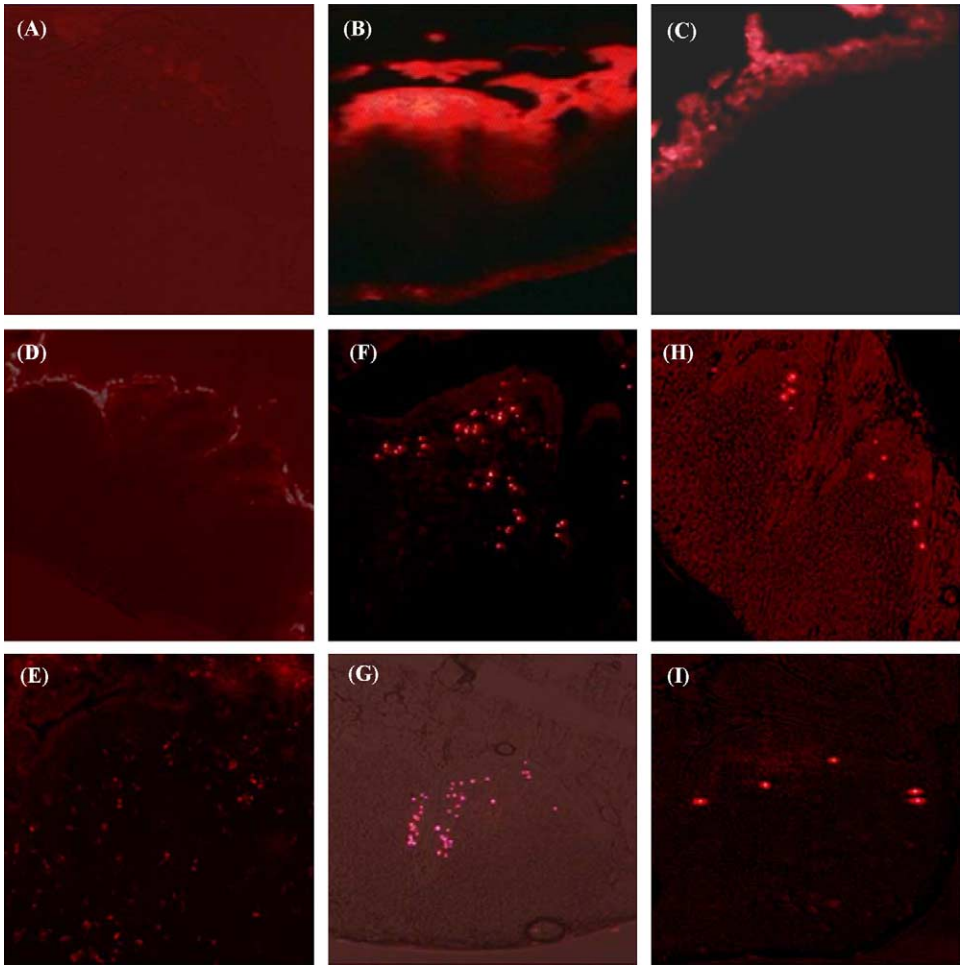

Fig. 4. Localisation of rhodamine microspheres in Peyer's patches after oral administration to mice. (A) non-treated mucosa. (B) Mucosa of animals fed with free rhodamine, 4 h after administration. (C) Mucosa of animals fed with free rhodamine, 24 h after administration. (D) 0.3 μm nanospheres, 4 h after administration. (E) 0.3 μm nanospheres, 24 h after administration. (F) 1 μm microspheres, 4 h after administration. (G) 1 μm microspheres, 24 h after administration. (H) 3–5 μm microspheres, 4 h after administration. (I) 3–5 μm microspheres, 24 h after administration.

their 0.3 and 1 μm counterparts. The finding that the particles with a size equal or less than 1 μm were more efficiently taken up by the Peyer's patches is in agreement with previous studies performed with latex microspheres (Jani et al., 1989) and with particles of poly(lactide) (McClean et al., 1998). The maximum number of particles in the PPs was counted 4 h after administration. This number diminished significantly 48 h after administration (Fig. 3) due probably to the property of the smaller particles being removed from PPs by passage through lymph nodes and thoracic duct (Eldridge et al., 1990; Jani et al., 1989).

3.3. Depletion of gut-associated macrophages and oral contamination with TSE

The gut-associated macrophages were depleted using the macrophage-suicide technique. Mice were treated twice with microparticles (of the same size as those previously tested) loaded with of clodronate,

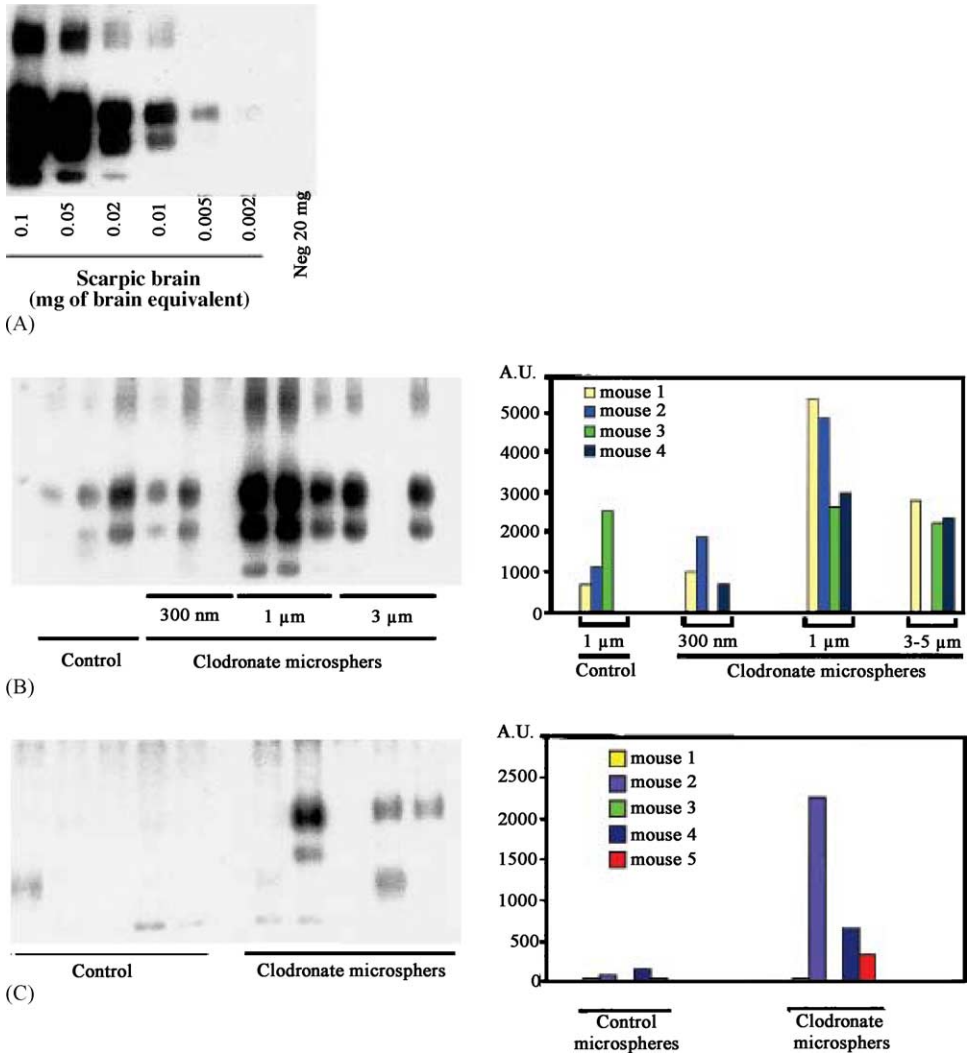

Fig. 5. PrPres detection in the Peyer's patches of mice orally infected with BSE or scrapie. (A) Dilution scale of PrPres in the brain of mice at terminal stage of scrapie (positive control for PrPres detection) (B) 130 days post-inoculation, scrapie strain C506M3. (C) 60 days post-inoculation, BSE strain 6PB1. Clodronate microspheres 1 μm were used. Control microspheres were clodronate unloaded PLGA microspheres. Bars represent the quantification of the Western-blot signal using the NIH Image program.

three and two days before the oral contamination with the mouse-adapted scrapie (C506M3) strain. Peyer's patches were harvested at 130 days post-infection (dpi) and assayed for PrPres accumulation by Western-blot using the JB007 polyclonal PrP antibody (Maignien et al., 1999). Fig. 5B shows that microspheres of 1 μm average diameter increased significantly the PrPres content of the Peyer's patches when compared to unloaded control microspheres ($p = 0.0209$, Mann–Whitney test), while only a slight effect was seen with the 3–5 μm microspheres. In contrast, no detectable effect was seen using 0.3 μm nanospheres although these particles were visible in the Peyer's patches. This could be explained by the too rapid release of clodronate from nanoparticles before being taken up by Peyer's patches (Fig. 2).

To verify whether or not the observed phenomenon was strain-specific we applied the treatment using the

1 μm microspheres to mice inoculated with the BSE strain 6PB1 (Lasmezas et al., 1996). Fig. 5C shows that, at 60 dpi, PrPres was only barely detectable in one out of five mice treated with control microspheres, whereas significant amounts of PrPres were present in three out of five clodronate-treated mice. Thus, the clodronate treatment increased PrPres accumulation in this model as well. In a previous study, we had shown that the pathogenesis of the oral route of infection differed in scrapie and BSE in that in the former, PrPres was distributed throughout the intestinal tract from the stomach to the rectum, while in the latter,

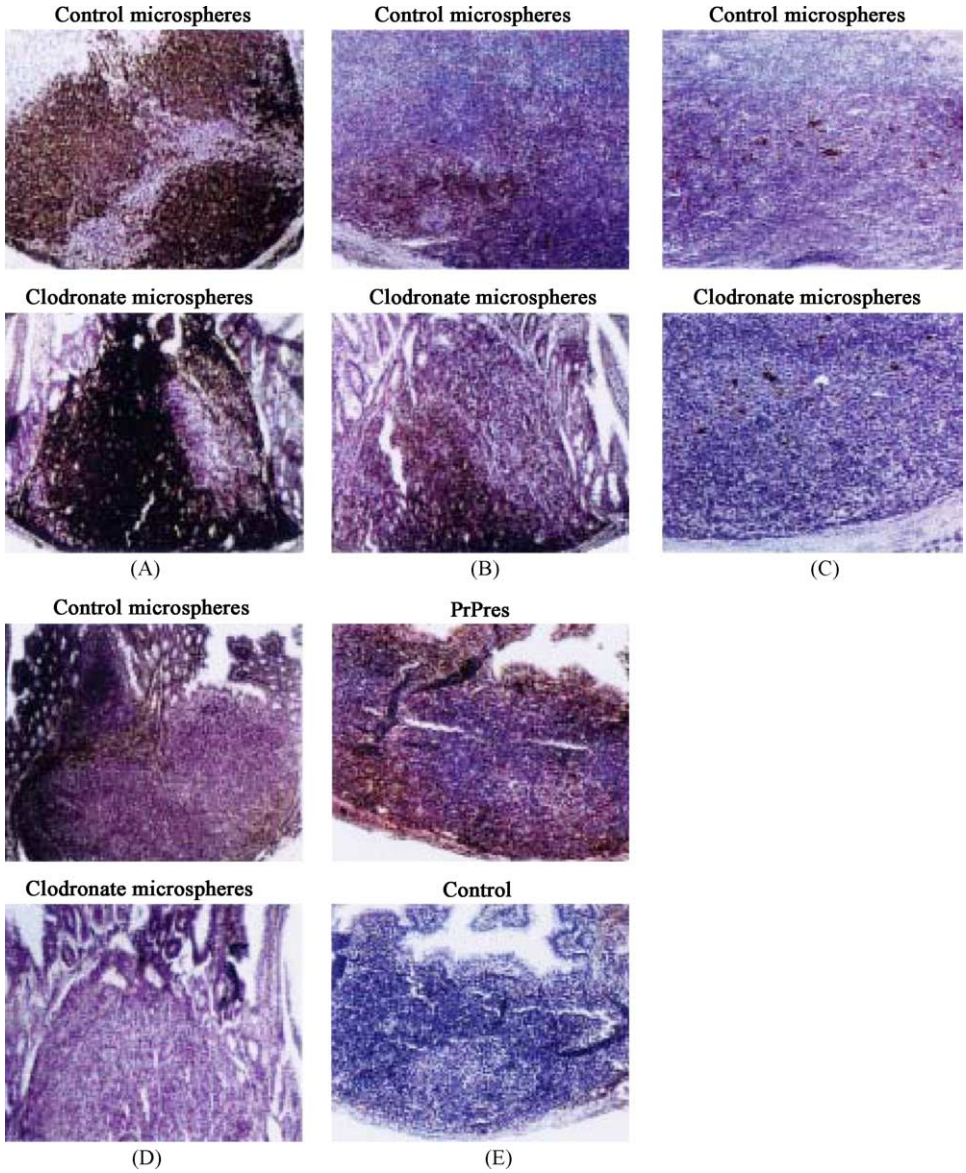

Fig. 6. Immunohistochemistry of dissected Peyer's patches (A) B lymphocyte labelling (B220 Ab) (B) T lymphocyte labelling (CD3e Ab) (C) follicular dendritic cell labelling (FDC-M1 Ab) (D) macrophage labelling (F4/80 Ab) (E) PrP deposits at terminal stage in infected mice (monoclonal antibody SAF60, control with secondary antibody).

PrPres accumulation was restricted to the Peyer's patches (Maignien et al., 1999). Thus, the observation that clodronate exerts an effect in the BSE model as well, tends to support our original assumption that the mechanism of action of clodronate is specifically related to its localisation in the domes of PPs.

3.4. Immunohistochemistry

We then tried to correlate the observed impediment of PrPres generation with the effect of clodronate microspheres on the cell populations in the intestinal domes. Thus, cells were characterized immunohistochemically 48 h after the treatment to allow cell deprivation to occur (which corresponds to the time of oral challenge with the infectious agents). Fig. 6A shows that the main cell population of the follicles consisted of B-lymphocytes labelled with a B220 antibody. T lymphocytes recognized by a CD3e antibody had a more restricted localization at the periphery of the follicles (Fig. 6B). B and T cell populations appeared to be unaffected by the microsphere treatment. FDCs decorated with FDC-M1, as well as morphologically recognizable body macrophages were also present to the same extent in treated and non-treated animals; they formed clusters in the center of the germinal centers (Fig. 6C). However, F4/80 labelled macrophages, which were present in the surroundings of the follicles of all PPs in the control animals, were absent from most of them in treated mice (Fig. 6D). It is noteworthy that the PrP deposits observed in animals at late stage of the disease after oral infection were seen not only in the center of the germinal center but also colocalizing with the macrophage labelling on the periphery of the follicles (Fig. 6E).

FDCs play a central role in TSE pathogenesis as artificially created chimeric mice harbouring a functional immune system but lacking PrPc expression on the surface of FDCs do not replicate prions in their spleen (Brown et al., 1999). Our data show that a treatment which respects the integrity of this cell population while inducing a severe deprivation of cells from the monocyte/macrophage lineage located at the interface between the gut epithelium and the follicles accelerates the early steps of infection, as PrPres appeared earlier in the gut-associated lymphoid tissue. The fact that PrPres levels were still higher at 130 days post-infection, when PrPres was already detectable in untreated animals, shows that the accumulation process of the protein, closely correlated with the pace of agent replication in the stabilized experimental models of TSEs used in this study: it occurs at a steady rate once initiated. Thus, a certain amount of infectious agent reaches the germinal centers containing the FDCs, and from this starting pool, replication occurs according to a clockwise-regulated process. Thus, the role of the macrophages in this pathogenetical set-up seems to clear a certain amount of the agent that has crossed the gut barrier. The remaining quantity of infectious particles, if above the threshold for infection, then determines the whole kinetics of the disease process.

4. Conclusion

This study has contributed to unveiling the role of gut-associated macrophages in the initial clearance of infectious particles that have passed the first hurdle of the gut barrier. Together with cells responsible for the transport of the agent from the lumen to the post-epithelial compartment, the role of the macrophages from the periphery of the follicles is, therefore, a key parameter as they define the actual infectious dose determining the subsequent kinetics of infection. These cells may play additional roles, too in the propagation of the infectious agent during the later steps of the infection. This deserves to be further investigated by appropriate functional approaches.

Acknowledgements

We gratefully acknowledge the expert care of the animals provided by René Rioux. We thank M. Kosko-Vilbois for provision of the FDC-M1 antibody. This work has been funded by the European Union (Grant BMH4-CT98-3265). T.M. is a recipient of fellowship from Fondation MERIEUX (17 rue Bourgelat BP 2021 69227 LYON cedex 02).

References

Beekes, M., McBride, P.A., 2000. Early accumulation of pathological PrP in the enteric nervous system and gut-associated lymphoid tissue of hamsters orally infected with scrapie. Neurosci. Lett. 278, 181–184.

Beringue, V., Demoy, M., Lasmezas, C.I., Gouritin, B., Weingarten, C., Deslys, J.P., Andreux, J.P., Couvreur, P., Dormont, D., 2000. Role of spleen macrophages in the clearance of scrapie agent early in pathogenesis. J. Pathol. 190, 495–502.

Brown, K.L., Stewart, K., Ritchie, D.L., Mabbott, N.A., Williams, A., Fraser, H., Morrison, W.I., Bruce, M.E., 1999. Scrapie replication in lymphoid tissues depends on prion protein-expressing follicular dendritic cells. Nat. Med. 5, 1308–1312.

Bruce, M.E., Will, R.G., Ironside, J.W., McConnell, I., Drummond, D., Suttie, A., McCardle, L., Chree, A., Hope, J., Birkett, C., Cousens, S., Fraser, H., Bostock, C.J., 1997. Transmissions to mice indicate that 'new variant' CJD is caused by the BSE agent. Nature 389, 498–501.

Demaimay, R., Adjou, K.T., Beringue, V., Demart, S., Lasmezas, C.I., Deslys, J.P., Seman, M., Dormont, D., 1997. Late treatment with polyene antibiotics can prolong the survival time of scrapie-infected animals. J. Virol. 71, 9685–9689.

Eldridge, J.H., Hammond, C.J., Meulbroek, J.A., Staas, J.K., Gilley, R.M., Tice, T.R., 1990. Controlled vaccine release in the gut-associated lymphoid tissues. I. Orally administered biodegradable microspheres target the peyer's patches. J. Control. Release 11, 205–214.

Fraser, H., Farquhar, C.F., McConnell, I., Davies, D., 1989. The scrapie disease process is unaffected by ionising radiation. Prog. Clin. Biol. Res. 317, 653–658.

Hill, A.F., Desbruslais, M., Joiner, S., Sidle, K.C., Gowland, I., Collinge, J., Doey, L.J., Lantos, P., 1997. The same prion strain causes vCJD and BSE. Nature 389, 448–450, 526.

Jani, P., Halbert, G.W., Langridge, J., Florence, A.T., 1989. The uptake and translocation of latex nanospheres and microspheres after oral administration to rats. J. Pharm. Pharmacol. 41, 809–812.

Jeffrey, M., McGovern, G., Goodsir, C.M., Brown, K.L., Bruce, M.E., 2000. Sites of prion protein accumulation in scrapie-infected mouse spleen revealed by immuno-electron microscopy. J. Pathol. 191, 323–332.

Kimberlin, R.H., Walker, C.A., 1989. Pathogenesis of scrapie in mice after intragastric infection. Virus Res. 12, 213–220.

Kitamoto, T., Muramoto, T., Mohri, S., Doh-Ura, K., Tateishi, J., 1991. Abnormal isoform of prion protein accumulates in follicular dendritic cells in mice with Creutzfeldt–Jakob disease. J. Virol. 65, 6292–6295.

Klein, M.A., Frigg, R., Flechsig, E., Raeber, A.J., Kalinke, U., Bluethmann, H., Bootz, F., Suter, M., Zinkernagel, R.M., Aguzzi, A., 1997. A crucial role for B cells in neuroinvasive scrapie. Nature 390, 687–690.

Lasmezas, C.I., Deslys, J.P., Demaimay, R., Adjou, K.T., Hauw, J.J., Dormont, D., 1996. Strain specific and common pathogenic events in murine models of scrapie and bovine spongiform encephalopathy. J. Gen. Virol. 77, 1601–1609.

Lasmezas, C.I., Deslys, J.P., Robain, O., Jaegly, A., Beringue, V., Peyrin, J.M., Fournier, J.G., Hauw, J.J., Rossier, J., Dormont, D., 1997. Transmission of the BSE agent to mice in the absence of detectable abnormal prion protein. Science 275, 402–405.

Lasmezas, C.I., Fournier, J.G., Nouvel, V., Boe, H., Marce, D., Lamoury, F., Kopp, N., Hauw, J.J., Ironside, J., Bruce, M., Dormont, D., Deslys, J.P., 2001. Adaptation of the bovine spongiform encephalopathy agent to primates and comparison with Creutzfeldt–Jakob disease: implications for human health. Proc. Natl. Acad. Sci. U.S.A. 98, 4142–4147.

Mabbott, N.A., Mackay, F., Minns, F., Bruce, M.E., 2000. Temporary inactivation of follicular dendritic cells delays neuroinvasion of scrapie. Nat. Med. 6, 719–720.

Maignien, T., Lasmezas, C.I., Beringue, V., Dormont, D., Deslys, J.P., 1999. Pathogenesis of the oral route of infection of mice with scrapie and bovine spongiform encephalopathy agents. J. Gen. Virol. 80, 3035–3042.

Manuelidis, L., Zaitsev, I., Koni, P., Lu, Z.Y., Flavell, R.A., Fritch, W., 2000. Follicular dendritic cells and dissemination of Creutzfeldt–Jakob disease. J. Virol. 74, 8614–8622.

McBride, P.A., Beekes, M., 1999. Pathological PrP is abundant in sympathetic and sensory ganglia of hamsters fed with scrapie. Neurosci. Lett. 265, 135–138.

McBride, P.A., Eikelenboom, P., Kraal, G., Fraser, H., Bruce, M.E., 1992. PrP protein is associated with follicular dendritic cells of spleens and lymph nodes in uninfected and scrapie-infected mice. J. Pathol. 168, 413–418.

McClean, S., Prosser, E., Meehan, E., O'Malley, D., Clarke, N., Ramtoola, Z., Brayden, D., 1998. Binding and uptake of biodegradable poly(DL-lactide) micro- and nanoparticles in intestinal epithelia. Eur. J. Pharm. Sci. 6, 153–163.

Montrasio, F., Cozzio, A., Flechsig, E., Rossi, D., Klein, M.A., Rulicke, T., Raeber, A.J., Vosshenrich, C.A., Proft, J., Aguzzi, A., Weissmann, C., 2001. B lymphocyte-restricted expression of prion protein does not enable prion replication in prion protein knockout mice. Proc. Natl. Acad. Sci. U.S.A. 98, 4034–4037.

Montrasio, F., Frigg, R., Glatzel, M., Klein, M.A., Mackay, F., Aguzzi, A., Weissmann, C., 2000. Impaired prion replication in spleens of mice lacking functional follicular dendritic cells. Science 288, 1257–1259.

Shakweh, M., Ponchel, G., Fattal, E., 2004. Particle uptake by Peyer's patches: a pathway for drug and vaccine delivery. Exp. Opin. Drug Deliv. 1, 141–163.

Sigurdson, C.J., Williams, E.S., Miller, M.W., Spraker, T.R., O'Rourke, K.I., Hoover, E.A., 1999. Oral transmission and early lymphoid tropism of chronic wasting disease PrPres in mule deer fawns (*Odocoileus hemionus*). J. Gen. Virol. 80, 2757–2764.

van Keulen, L.J., Schreuder, B.E., Vromans, M.E., Langeveld, J.P., Smits, M.A., 1999. Scrapie-associated prion protein in the gastrointestinal tract of sheep with natural scrapie. J. Comp. Pathol. 121, 55–63.

Van Rooijen, N., 1989. The liposome-mediated macrophage 'suicide' technique. J. Immunol. Methods 124, 1–6.

Will, R.G., Ironside, J.W., Zeidler, M., Cousens, S.N., Estibeiro, K., Alperovitch, A., Poser, S., Pocchiari, M., Hofman, A., Smith, P.G., 1996. A new variant of Creutzfeldt–Jakob disease in the UK. Lancet 347, 921–925.